Mn-doped cubic BN as an atomiclike memory device: A density functional study

Antônio J. R. da Silva,[1,2,*] P. Piquini,[3] J. T. Arantes,[4] R. J. Baierle,[3] and A. Fazzio[1,5,†]
[1]*Instituto de Física, Universidade de São Paulo, CP 66318, 05315-970 São Paulo, SP, Brazil*
[2]*Laboratório Nacional de Luz Síncrotron, Campinas, SP, Brazil*
[3]*Departamento de Física, Universidade Federal de Santa Maria, 97105-900 Santa Maria, RS, Brazil*
[4]*Centro de Engenharia, Modelagem e Ciências Sociais Aplicadas, Universidade Federal do ABC, 09210-170 Santo André, SP, Brazil*
[5]*Centro de Ciências Naturais e Humanas, Universidade Federal do ABC, 09090-400 Santo André, SP, Brazil*
(Received 20 September 2009; revised manuscript received 7 April 2010; published 25 May 2010)

We investigate the electronic properties of Mn_B substitutional doping in cubic boron nitride (BN), for different charge states, using density functional theory (DFT) calculations. We show that the neutral Mn has a nonmagnetic ground state ($S=0$). Upon charge injection, it is unambiguously shown that the Mn_B^- has a high-spin configuration with a strong, localized magnetic moment of $5\mu_{Bohr}$. We developed a simple model, parameterized by the DFT results, that allows us to interpret the rules played by the crystal-field and exchange-correlation splitting in the magnetization process.

DOI: 10.1103/PhysRevB.81.195432 PACS number(s): 85.70.−w, 71.15.Nc, 71.55.Eq

I. INTRODUCTION

The challenge of increasing miniaturization of electronic devices has lead to prototypes of transistors and rectifiers based on, e.g., carbon nanotubes and silicon nanowires.[1–4] However, in order to have a fully operational nanoscale device, it is fundamental to have, in addition to the logical processing units, memory units that could store the processed information. One would like to have a memory unit that could easily have its state altered in order to have the information readily written or erased.

We here present a theoretical proposal of such a memory unit that (i) has strong magnetic moments localized in atomiclike regions centered on transition-metal impurities dispersed in a nonmagnetic host and (ii) can have its magnetic moment changed by the simple exchange of an electron, i.e., via the control of a charge current instead of a magnetic field. The system we investigate consists of a Mn impurity in a cation site of cubic BN (cBN). We show, via state of the art *ab initio* calculations, that this impurity in the neutral charge state has a zero magnetic moment whereas it changes to a strong local magnetic moment of $5\mu_{Bohr}$ when the Mn impurity captures one electron.

Ideas such as this one have already been realized for Au or Ag impurity atoms in insulating NaCl thin films,[5] and measurements and manipulation with atomic resolution are already a reality.[6–8] Moreover, it has been demonstrated experimentally the possibility of changing the magnetic properties of single Mn atoms in quantum dots by charge injection.[9] The zinc-blende phase of BN presents several interesting properties such as chemical inertness, extreme hardness, wide band gap, being easily doped both *p* and *n* type.[10] Great advances in the synthesis of this material showed that good-quality cBN samples can be grown through chemical vapor deposition on diamond substrates,[11] allowing both cBN-based electronic devices to be built in laboratories and theoretical predictions to be checked. It seems, therefore, a real possibility to dope this semiconductor with Mn atoms.

In the following section, we present the details of the performed calculations. In Sec. III, the results of the *ab initio* calculations are presented and discussed, as well as a density functional theory (DFT) parameterized simple model is developed and its results analyzed. Our conclusions end the Sec. III.

II. METHODOLOGY

All results were obtained through total-energy calculations based on *ab initio* spin-polarized DFT.[12] We used the PW91 generalized gradient approximation[13] to the exchange and correlation functional. Ultrasoft pseudopotentials[14] were employed to describe the interactions between the ionic cores and the valence electrons. A plane-wave expansion with a cutoff energy of 348 eV is used to represent the valence electrons. The Brillouin zone was sampled by a $3\times3\times3$ *k*-point mesh, according to the Monkhorst-Pack scheme.[15] A unit cell with 64 atoms was used to simulate each of the studied cBN:Mn systems, with the atoms relaxed until forces were lower than 0.001 eV/Å. For all considered charge states, we performed calculations taking both a fixed and a nonfixed value of the total spin of the supercell. For the spin-free calculations, whenever a Mn high-spin configuration was possible, it has also been taken into account as a possible initial guess.

In order to estimate the effects of the supercell size on the obtained results, we performed additional calculations for supercells with 54 and 128 atoms. It is observed that for the cases were the system has a nonzero magnetization, the resulting magnetic moments are still much localized around the Mn atoms. Further, the dispersion of the energy levels in the band structure is not significantly altered, and the energy difference between configurations with different total spin states remain the same within 0.05 eV.

III. RESULTS AND DISCUSSIONS

A. *Ab initio* results

We initially study a substitutional neutral Mn atom in a *B* site. We find that the Mn 3*d* levels are localized in the bulk band gap, which leads to a nominally Mn $3d^4$ configuration.

TABLE I. Relative energies for the different electronic configurations, associated with different total spins for the supercell, for the positively, neutral and negatively charged Mn impurity. The last column presents the projected weights α_{T_d} of the coordinates of the nearest neighbors to the Mn onto the symmetrized coordinate Q_{T_d}, as described in the text.

Charge state	Total spin	Elec. config.	Energy (eV)	α_{T_d}
(+1) ($3d^3$)	1/2	$e^3t_2^0$	0.0	0.39
	3/2	$e^2t_2^1$	0.31	0.45
(0) ($3d^4$)	0	$e^4t_2^0$	0.0	0.42
	1	$e^3t_2^1$	0.50	0.45
	2	$e^2t_2^2$	0.18	0.50
(−1) ($3d^5$)	1/2	$e^4t_2^1$	1.26	0.48
	3/2	$e^3t_2^2$	1.10	0.52
	5/2	$e^2t_2^3$	0.0	0.56

If no distortions are considered, the local symmetry around the Mn atom is tetrahedral. Therefore, the $3d$ orbitals centered on the ionic impurity can be classified according to the irreducible representations of the T_d point group, and the initially fivefold-degenerate $3d$ levels split into a low-lying twofold-degenerate e and a higher-energy threefold-degenerate t_2 subsets. The final state and, consequently, the total spin of the neutral as well as charged systems will be determined by the difference in the occupation numbers of the spin-up and spin-down levels.

For the neutral and charged substitutional Mn, we considered different electronic states which have distinct occupations and total spin configurations, as shown in Table I. These states are obtained by enforcing a given total occupation difference between the spin-up and spin-down channels in the supercell. An investigation of the local magnetization $m(\mathbf{r})=n_\uparrow(\mathbf{r})-n_\downarrow(\mathbf{r})$ indicates that it is mainly localized around the Mn atom. Thus, the different total supercell magnetic moments can actually be correlated with the above-mentioned Mn configurations. As an example of the degree of spatial localization of the magnetic moments in the Mn-doped cBN systems, the resulting magnetization for the negatively charged system is shown in Fig. 1. It is clearly seen from this figure that the magnetization is largely centered on the Mn impurity atom, decaying rapidly after its first neighbors. It emphasizes the almost atomic character of the resulting magnetic moment, and points to possible applications as charge controlled highly dense memory devices.

As can be seen in Table I, the lowest-energy state for the neutral Mn impurity corresponds to the low-spin configuration, $S=0$. The high-spin configuration ($S=2$) is higher in energy by 0.18 eV, followed by the $S=1$ state ($\Delta E^{1,0}=0.50$ eV). These energy differences depend on both crystal field and exchange interactions.[16] On the other hand, for the negatively charged state, we obtain that the high-spin state ($S=5/2$) has the lowest energy, followed by the $S=3/2$ ($\Delta E^{3/2,5/2}=1.10$ eV) and the $S=1/2$ ($\Delta E^{1/2,5/2}=1.26$ eV).[17] In Fig. 2, we show the spin-up and spin-down total density of states as well as the Mn d levels projected density of states

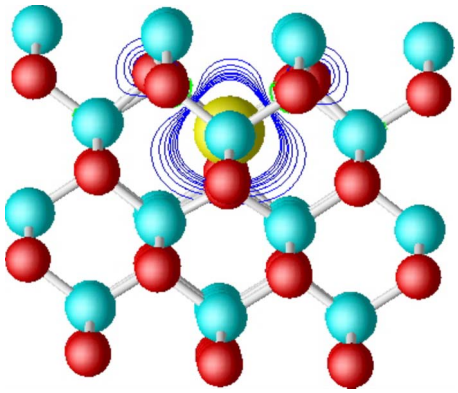

FIG. 1. (Color online) Contour plot of the resulting magnetization in the negatively charged Mn-doped cBN. The magnetization is centered on Mn impurity atom and decays abruptly after its first neighbors. The contour plot is taken at the [110] view and its isosurfaces are separated by 0.02 e/Å^3.

for the lowest-energy neutral of negatively charged states. It is clearly seen from this figure that the introduction of one electron abruptly changes the magnetization of the system. Similarly to the neutral charge state, the positively charged state has the low-spin configuration as the lowest-energy one.

The formation energies $E^q(\mu_e)$ of BN:Mn_B^q ($q=0,\pm1$), in the lowest-energy configurations for each charge state, can be calculated as $E^q(\mu_e)=E_{tot}^{\mathrm{Mn}^q}-E_{tot}^{pure}+\mu_B-\mu_{\mathrm{Mn}}+q(\mu_e+\varepsilon_v)$, where $E_{tot}^{\mathrm{Mn}^q}$ is the total energy of the supercell with a Mn in charge state q, E_{tot}^{pure} is the total energy of the perfect BN lattice supercell, μ_B and μ_{Mn} are the B and Mn chemical potentials, respectively, and μ_e is the position of the electronic chemical potential relative to the top of the valence band ε_v.

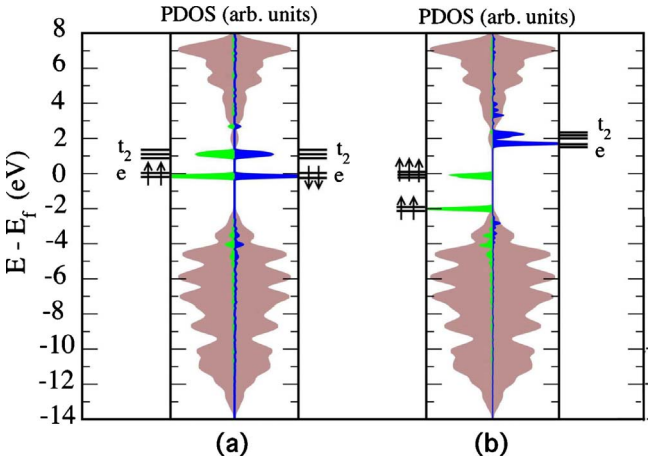

FIG. 2. (Color online) The spin-up (left side) and spin-down (right side) total density of states and Mn d levels projected density of states for the (a) neutral and (b) negatively charged Mn-doped (at a B site) cubic BN. The black horizontal lines indicate the Mn-derived e and t_2 levels with the respective electronic spin-up and spin-down occupations (indicate by vertical arrows). The Fermi level is at 0 eV.

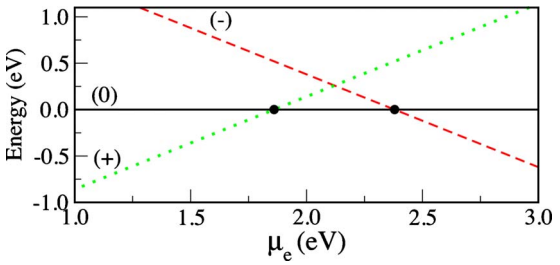

FIG. 3. (Color online) Relative formation energies for the different Mn charge states, as a function of the electronic chemical potential μ_e. The neutral charge state is taken as the reference.

In Fig. 3, we present the formation energies for each charge state q, as a function of μ_e, obtained using the above equation. However, as we are only interested in the values of the charge states' transition levels, we did not worry about the chemical potentials μ_B and μ_{Mn} since they will only change the absolute values but not the transition levels. From the curves of Fig. 3, we obtained the $(+/0)$ and the $(0/-)$ ionization levels, which are positioned at 1.86 and 2.38 eV above the valence-band maximum, respectively. From Fig. 3, we see that there is a narrow but comfortable energy window of $\simeq 0.52$ eV where the neutral state is the most stable configuration.

Each charge state of the Mn-doped cBN system will induce different relaxations on the host lattice. We have estimated these lattice relaxations by considering the undoped BN crystal as the reference configuration. The positions of the four nearest nitrogen neighbors to the Mn impurity atom can be described by a collective coordinate Q written as $Q = \alpha_{T_d} Q_{T_d} + \alpha_{D_{2d}} Q_{D_{2d}}$, where Q_{T_d} and $Q_{D_{2d}}$ are the symmetrized coordinates[18] that transform as the totally symmetric irreducible representations (A_1) of the T_d and D_{2d} point groups. The components α_{T_d} and $\alpha_{D_{2d}}$ can be obtained via a projection of the coordinates of the four nearest neighbors to the Mn onto the symmetrized coordinates Q_{T_d} and $Q_{D_{2d}}$. The calculated projected weights α_{T_d} are shown in Table I. We observe that the symmetry-breaking, Jahn-Teller distortions, are very small, and therefore do not discuss them any further. We also observe a systematic increase in the outward volume relaxation going from the (+) state toward the (−) one, which is consistent with the observed trend in the variation in the crystal-field splitting. Note as well that, for a given charge state, the higher-spin configurations have larger relaxations than the lower-spin ones. Thus, the crystal-field splitting (and most likely the exchange integral) is not constant for a given charge state.

We have calculated the stabilization energy of the charged states (relative to the neutral one) associated with the lattice relaxations. It has been calculated by the total-energy difference between the configuration of the neutral state with an additional charge, and the completely relaxed configuration of the respective charged state. These stabilization energies for the most stable configurations of the negatively and positively charged states are 0.55 eV and 0.12 eV, respectively.

B. DFT parameterized model

In order to rationalize the results from the *ab initio* calculations, we propose a simplified model which takes into account the two main contributions that will determine the relative stability of the different total spin states for each charge state of the Mn-doped cBN: (i) crystal-field splitting and (ii) exchange interactions.

Starting from the Kohn-Sham (KS) equations $\{-\frac{1}{2}\nabla^2 + V_{ion} + V_{xc}[n(\mathbf{r})] + V_H[n(\mathbf{r})]\}\phi_\alpha = \varepsilon_\alpha \phi_\alpha$, where the terms represent the kinetic-energy, the ionic, exchange-correlation, and Hartree potentials, respectively, let us take the set of KS orbitals that have a strong Mn d-orbitals character, which are rather localized around the Mn ion. Let us denote these orbitals $\{\phi^{i,\sigma}_{\mathrm{Mn}_d}\}$ with $i=1-5$ and $\sigma=\uparrow,\downarrow$. We now write the ionic potential as $V_{ion} = V^{crystal}_{ion} + V^{\mathrm{Mn}}_{ion}$ and the total density as $n(\mathbf{r}) = n_{crystal}(\mathbf{r}) + n_{\mathrm{Mn}_d}(\mathbf{r})$, where $V^{crystal}_{ion}$ is the ionic potential caused by all the ions but the Mn, which has an ionic potential V^{Mn}_{ion}, and $n_{\mathrm{Mn}_d}(\mathbf{r}) = \Sigma_{\{i,\sigma\}} f_{i,\sigma} \phi^{*i,\sigma}_{\mathrm{Mn}_d} \phi^{i,\sigma}_{\mathrm{Mn}_d}$, where $f_{i,\sigma}$ is the occupation of orbital $\phi^{i,\sigma}_{\mathrm{Mn}_d}$.

With this separation, the Hartree potential can be exactly written as $V_H(n) = V^{crystal}_H(n_{crystal}) + V^{\mathrm{Mn}_d}_H(n_{\mathrm{Mn}_d})$. The exchange-correlation potential, on the other hand, due to its nonlinear character, cannot be exactly separated. However, if the overlap between the crystal and the Mn_d densities is small, we can approximately write $V_{xc}(n) \approx V^{crystal}_{xc}(n_{crystal}) + V^{\mathrm{Mn}_d}_{xc}(n_{\mathrm{Mn}_d})$. With all these approximations and definitions, we can write for the eigenvalues $\varepsilon^{i,\sigma}_{\mathrm{Mn}_d}$,

$$\varepsilon^{i,\sigma}_{\mathrm{Mn}_d} = \left\{ \int \{V^{crystal}_{ion}(\mathbf{r}) + V^{crystal}_H[n_{crystal}(\mathbf{r})] + V^{crystal}_{xc}[n_{crystal}(\mathbf{r})]\} n^{i,\sigma}_{\mathrm{Mn}_d}(\mathbf{r}) d\mathbf{r} \right\} + \left\{ \int \phi^{*i,\sigma}_{\mathrm{Mn}_d}(\mathbf{r}) \left(-\frac{1}{2}\nabla^2 \right) \phi^{i,\sigma}_{\mathrm{Mn}_d}(\mathbf{r}) d\mathbf{r} + \int \{V^{\mathrm{Mn}}_{ion}(\mathbf{r}) + V^{\mathrm{Mn}_d}_H[n_{\mathrm{Mn}_d}(\mathbf{r})] + V^{\mathrm{Mn}_d}_{xc}[n_{\mathrm{Mn}_d}(\mathbf{r})]\} n^{i,\sigma}_{\mathrm{Mn}_d}(\mathbf{r}) d\mathbf{r} \right\}. \quad (1)$$

Let us now consider two different Mn configurations, i.e., different populations in the e and t_2 levels, that will have two distinct densities $n^{(1)} = n_{crystal} + n^{(1)}_{\mathrm{Mn}_d}$ and $n^{(2)} = n_{crystal} + n^{(2)}_{\mathrm{Mn}_d}$, which we are assuming differ only in the n_{Mn_d} part. Considering now the total energy,

$$E_{tot}[n] = \sum_{\alpha} \varepsilon_{\alpha} - \frac{1}{2}\int \frac{n(\mathbf{r}')n(\mathbf{r})}{|\mathbf{r}-\mathbf{r}'|} d\mathbf{r}' d\mathbf{r} + E_{xc}[n] - \int V_{xc}[n(\mathbf{r})] \times n(\mathbf{r}) d\mathbf{r} \tag{2}$$

and writing for the sum of KS eigenvalues $\Sigma_{\alpha}\varepsilon_{\alpha}^{(1)} = \Sigma_{\alpha}\varepsilon_{\alpha}^{crystal} + \Sigma_{i,\sigma}\varepsilon_{\mathrm{Mn}_d}^{(1)i,\sigma}$ and $\Sigma_{\alpha}\varepsilon_{\alpha}^{(2)} = \Sigma_{\alpha}\varepsilon_{\alpha}^{crystal} + \Sigma_{i,\sigma}\varepsilon_{\mathrm{Mn}_d}^{(2)i,\sigma}$, we can express the total-energy difference between the two configurations, $\Delta E^{(2,1)} = E_{tot}^{(2)}[n^{(2)}] - E_{tot}^{(1)}[n^{(1)}]$, as

$$\Delta E^{(2,1)} = \int V_{ion}^{crystal}(\mathbf{r})[n_{\mathrm{Mn}_d}^{(2)}(\mathbf{r}) - n_{\mathrm{Mn}_d}^{(1)}(\mathbf{r})]d\mathbf{r} + T_s[n_{\mathrm{Mn}_d}^{(2)}] - T_s[n_{\mathrm{Mn}_d}^{(1)}] + E_{xc}[n_{\mathrm{Mn}_d}^{(2)}] - E_{xc}[n_{\mathrm{Mn}_d}^{(1)}] + \int V_{ion}^{\mathrm{Mn}}(\mathbf{r}) \times [n_{\mathrm{Mn}_d}^{(2)}(\mathbf{r}) - n_{\mathrm{Mn}_d}^{(1)}(\mathbf{r})]d\mathbf{r}$$
$$+ \frac{1}{2}\int \frac{n_{\mathrm{Mn}_d}^{(2)}(\mathbf{r})n_{\mathrm{Mn}_d}^{(2)}(\mathbf{r}') - n_{\mathrm{Mn}_d}^{(1)}(\mathbf{r})n_{\mathrm{Mn}_d}^{(1)}(\mathbf{r}')}{|\mathbf{r}-\mathbf{r}'|} d\mathbf{r}d\mathbf{r}' + \int n_{crystal}\{V_{xc}(n_{\mathrm{Mn}_d}^{(1)}) - V_{xc}(n_{\mathrm{Mn}_d}^{(2)})\}d\mathbf{r}, \tag{3}$$

where $T_s[n_X]$ is the Kohn-Sham kinetic-energy functional of a system with electronic density n_X.

We have assumed, in order to obtain the above expressions, that (1) $\Sigma_{\alpha}\varepsilon_{\alpha}^{crystal}$ is the same for both configurations and (2) $E_{xc}[n^{(i)}] \approx E_{xc}[n_{crystal}] + E_{xc}[n_{\mathrm{Mn}_d}^{(i)}]$. We may now define the total energy of a Mn ion in a given configuration as

$$E_{tot}^{\mathrm{Mn}_d(i)} = T_s[n_{\mathrm{Mn}_d}^{(i)}] + \int V_{ion}^{\mathrm{Mn}_d}(\mathbf{r})n_{\mathrm{Mn}_d}^{(i)}(\mathbf{r})d\mathbf{r} + \frac{1}{2}\int \frac{n_{\mathrm{Mn}_d}^{(i)}(\mathbf{r})n_{\mathrm{Mn}_d}^{(i)}(\mathbf{r}')}{|\mathbf{r}-\mathbf{r}'|} d\mathbf{r}d\mathbf{r}' + E_{xc}[n_{\mathrm{Mn}_d}^{(i)}], \tag{4}$$

which allows us to rewrite Eq. (3) as

$$\Delta E^{(2,1)} = \int V_{ion}^{crystal}(\mathbf{r})[n_{\mathrm{Mn}_d}^{(2)}(\mathbf{r}) - n_{\mathrm{Mn}_d}^{(1)}(\mathbf{r})]d\mathbf{r} + [E_{tot}^{\mathrm{Mn}_d(2)} - E_{tot}^{\mathrm{Mn}_d(1)}] + \int n_{crystal}(\mathbf{r})[V_{xc}(n_{\mathrm{Mn}_d}^{(1)}) - V_{xc}(n_{\mathrm{Mn}_d}^{(2)})]d\mathbf{r}. \tag{5}$$

Therefore, we show that the total-energy difference between two configurations of a Mn impurity in the crystal has three contributions: (i) a crystal-field term with an electrostatic character. It is the difference between the effect of the ionic crystal potential acting on the localized Mn charge-density distributions for the two configurations; (ii) an intramanganese total-energy difference; and (iii) a term also related to the crystal influence on the Mn ions. This term, however, is much smaller than the other two since it involves an overlap between the crystal charge density and the difference in exchange-correlation potentials for the Mn ions. As this latter potential difference is rather localized, the overall integral is much smaller than the other two terms. Thus, we can write $\Delta E^{(2,1)} \approx \Delta_{CF} + \Delta E_{\mathrm{Mn}_d}^{(2,1)}$, where $\Delta_{CF} = \int V_{ion}^{crystal}(\mathbf{r})[n_{\mathrm{Mn}_d}^{(2)}(\mathbf{r}) - n_{\mathrm{Mn}_d}^{(1)}(\mathbf{r})]d\mathbf{r}$ and $\Delta E_{\mathrm{Mn}_d}^{(2,1)} = [E_{tot}^{\mathrm{Mn}_d(2)} - E_{tot}^{\mathrm{Mn}_d(1)}]$.

We can now approximate the crystal-field Hamiltonian as $H_{CF} \approx (\varepsilon_d - \frac{3}{5}\delta_{CF})\hat{n}_e + (\varepsilon_d + \frac{2}{5}\delta_{CF})\hat{n}_{t_2}$, where ε_d is the Mn-ion d level, δ_{CF} is the crystal-field splitting between the e and t_2 levels, and $\hat{n}_e$ and $\hat{n}_{t_2}$ are the number operators for the e and t_2 levels, respectively. If the two distinct Mn configurations are represented by the states $|\mathrm{Mn}_d^{(1)}\rangle$ and $|\mathrm{Mn}_d^{(2)}\rangle$, then

$$\Delta_{CF} = \langle \mathrm{Mn}_d^{(2)}|H_{CF}|\mathrm{Mn}_d^{(2)}\rangle - \langle \mathrm{Mn}_d^{(1)}|H_{CF}|\mathrm{Mn}_d^{(1)}\rangle = \left\{ \frac{2}{5}\delta_{CF}[N_{t_2}^{(2)} - N_{t_2}^{(1)}] - \frac{3}{5}\delta_{CF}[N_e^{(2)} - N_e^{(1)}] \right\}, \tag{6}$$

where $N_e^{(i)}$ and $N_{t_2}^{(i)}$ are the total number of electrons occupying the e and t_2 levels, respectively, in the state $|\mathrm{Mn}_d^{(i)}\rangle$. The Hamiltonian for the Mn ion can be written as $H_{\mathrm{Mn}_d} \approx \Sigma_{i,\sigma}\varepsilon_d a_{i,\sigma}^{\dagger}a_{i,\sigma} + \Sigma_{ijkl,\sigma\sigma'}U_{ijkl}a_{i,\sigma}^{\dagger}a_{j,\sigma'}^{\dagger}a_{k,\sigma'}a_{l,\sigma}$, where $a_{i,\sigma}^{\dagger}(a_{i,\sigma})$ create (annihilate) an electron in the Mn d level (i,σ). If we consider the average energy in the Mn configuration $|\mathrm{Mn}_d^{(i)}\rangle$, we have

$$\langle \mathrm{Mn}_d^{(i)}|H_{\mathrm{Mn}_d}|\mathrm{Mn}_d^{(i)}\rangle = \sum_i U_{ii}n_{i\uparrow}n_{i\downarrow} + \frac{1}{2}\sum_{ij,i\neq j} U_{ij}(n_{i\uparrow} + n_{i\downarrow}) \times (n_{j\uparrow} + n_{j\downarrow}) - \frac{1}{2}\sum_{ij,i\neq j} J_{ij}(n_{i\uparrow}n_{j\uparrow} + n_{i\downarrow}n_{j\downarrow}), \tag{7}$$

where $U_{ii} = U_{iiii}$, $U_{i,j} = U_{ijij}$, and $J_{i,j} = U_{ijji}$. If we now make the assumption that the effective Coulomb and exchange energies are the same for all the e and t_2 orbitals, i.e., $U_{ii} = U_{ij} = U$ and $J_{ij} = K$, which is reasonable since we only want to provide an explanation of the *ab initio* results via a simple effective Hamiltonian with the fewer possible number of parameters, we have

$$\langle \mathrm{Mn}_d^{(i)}|H_{\mathrm{Mn}_d}|\mathrm{Mn}_d^{(i)}\rangle = \frac{N(N-1)}{2}U - \frac{1}{2}K[N_{\uparrow}(N_{\uparrow}-1) + N_{\downarrow}(N_{\downarrow}-1)]. \tag{8}$$

In the above expression, N is the total number of electrons in the Mn_d levels and $N_{\uparrow}$ $(N_{\downarrow})$ is the total number of up (down) electrons in the Mn_d levels. For the Mn_B^q in a given charge state q, N is the same for all configurations. Therefore,

$$\Delta E^{(2,1)} = -\frac{K}{2}\{[N_{\uparrow}^{(2)}(N_{\uparrow}^{(2)}-1) + N_{\downarrow}^{(2)}(N_{\downarrow}^{(2)}-1)] - [N_{\uparrow}^{(1)}(N_{\uparrow}^{(1)}-1) + N_{\downarrow}^{(1)}(N_{\downarrow}^{(1)}-1)]\} + \Delta_{CF}. \tag{9}$$

TABLE II. Energy differences, $\Delta E^{S_2,S_1}$, between different electronic configurations associated with different total spins S_2 and S_1, for the positively, neutral, and negatively charged Mn impurity. The expressions are obtained via Eq. (9). The effective parameters δ_{CF} and K are obtained using the total-energy results from Table I.

Charge	$\Delta E^{S_2,S_1}$		δ_{CF} (eV)	K (eV)
(0)	$\Delta E^{1,0}$	$\Delta E^{2,0}$		
	$\delta_{CF}-K$	$2\delta_{CF}-4K$	0.91	0.41
(−1)	$\Delta E^{3/2,5/2}$	$\Delta E^{1/2,5/2}$		
	$-\delta_{CF}+4K$	$-2\delta_{CF}+6K$	0.78	0.47

Thus, we obtain a simple expression that has only two parameters, δ_{CF} and K, where δ_{CF} is defined in Eq. (6). Even though many approximations were made in the derivation of Eq. (9), one should note that its main purpose is to provide means to rationalize, from the *ab initio* results, the competition between the two main contributions to the energy differences for a given charge state, the crystal-field splitting and the exchange energy. In Table II, we present these effective parameters obtained from the *ab initio* results of Table I. For the neutral charge state, we obtain a crystal-field splitting δ_{CF} that is more than twice as large as the effective exchange energy K. As can be deduced from Eq. (9), in order to have the low-spin and high-spin states with the same energy, we need to have $\delta_{CF}=2K$. If $\delta_{CF}<2K$, the high-spin configuration is favored. Otherwise, the low-spin state becomes the ground state. This is precisely what happens for the neutral substitutional Mn in cBN. Note, however, that as $\delta_{CF}\gtrsim 2K$, there is only a slight energy difference between the high- and low-spin states ($\simeq 0.2$ eV).

For the negatively charged state, there is a decrease in the crystal-field splitting δ_{CF} and a slight increase in the exchange integral K when compared to the neutral state in such a way that now $\delta_{CF}<2K$. Thus, we show that by "injecting" charge in the Mn ion, there is a dramatic change in the magnetic moment, going from $S=0$ for the neutral state to $S=5/2$ for the negative state. To our knowledge, this huge variation in the magnetization, from zero to $5\mu_{Bohr}$, with the addition of just one electron is unique among bulk materials.

For the positively charged state, on the other hand, we cannot extract the parameters δ_{CF} and K separately, only the combination $\delta_{CF}-2K$, which we know to be equal to $\delta_{CF}-2K=0.31$ eV. However, in order to have an estimate of the strength of these parameters, we chose the same value as for the neutral charge state, $K=0.4$ eV. With this choice, $\delta_{CF}=1.1$ eV. Thus, we see that there is a tendency toward an increase in the crystal-field splitting as the system goes from the negatively to the positively charged state. This increase is most likely caused by different lattice relaxations around the Mn ion.

In summary, we have shown that an isolated Mn substitutional impurity in a cBN matrix may be used as a memory storage media, with a huge variation of $5\mu_{Bohr}$ in the magnetic moment when going from the neutral (nonmagnetic, with a fully occupied e orbital) to the negatively charged state. This possibility of controlling the magnetic moment simply by charge injection is a very nice feature in the design of nanoscale memory devices.

ACKNOWLEDGMENTS

We acknowledge support from FAPESP, FAPERGS, and CNPq, and the CENAPAD-SP for computer time.

*ajrsilva@if.usp.br
†fazzio@if.usp.br

[1] S. J. Tans, A. R. M. Verschueren, and C. Dekker, Nature (London) **393**, 49 (1998).
[2] A. Bachtold, P. Hadley, T. Nakanishi, and C. Dekker, Science **294**, 1317 (2001).
[3] Y. Cui and C. M. Lieber, Science **291**, 851 (2001).
[4] Y. Cui, Z. Zhong, D. Wang, W. U. Wang, and C. M. Lieber, Nano Lett. **3**, 149 (2003).
[5] J. Repp, G. Meyer, F. E. Olsson, and M. Persson, Science **305**, 493 (2004); F. E. Olsson, S. Paavilainen, M. Persson, J. Repp, and G. Meyer, Phys. Rev. Lett. **98**, 176803 (2007).
[6] A. J. Heinrich, J. A. Gupta, C. P. Lutz, and D. M. Eigler, Science **306**, 466 (2004).
[7] C. F. Hirjibehedin, C.-Y. Lin, A. F. Otte, M. Ternes, C. P. Lutz, B. A. Jones, and A. J. Heinrich, Science **317**, 1199 (2007).
[8] P. Gambardella, S. Rusponi, M. Veronese, S. S. Dhesi, C. Grazioli, A. Dallmeyer, I. Cabria, R. Zeller, P. H. Dederichs, K. Kern, C. Carbone, and H. Brune, Science **300**, 1130 (2003).
[9] Y. Léger, L. Besombes, J. Fernández-Rossier, L. Maingault, and H. Mariette, Phys. Rev. Lett. **97**, 107401 (2006).
[10] P. B. Mirkarimi, K. F. McCarty, and D. L. Medlin, Mater. Sci. Eng. R. **21**, 47 (1997).
[11] X. W. Zhang, H.-G. Boyen, N. Deineka, P. Ziemann, F. Banhart, and M. Schreck, Nature Mater. **2**, 312 (2003).
[12] G. Kresse and J. Hafner, Phys. Rev. B **47**, 558 (1993); G. Kresse and J. Furthmüller, *ibid.* **54**, 11169 (1996).
[13] J. P. Perdew and Y. Wang, Phys. Rev. B **45**, 13244 (1992).
[14] D. Vanderbilt, Phys. Rev. B **41**, 7892 (1990).
[15] H. J. Monkhorst and J. D. Pack, Phys. Rev. B **13**, 5188 (1976).
[16] It should be noted that the GGA exchange functional used can be still improved by, e.g., exact exchange approaches. However, the energy differences obtained for the different spin states are not so small, and we believe that the main conclusions of our results will be maintained even if more elaborate approaches to the exchange interaction are employed.
[17] Mn impurities in BN have also been studied by L. V. C. Assali, W. V. M. Machado, and J. F. Justo, Appl. Phys. Lett. **89**, 072102 (2006).
[18] A. Fazzio, A. Janotti, A. J. R. da Silva, and R. Mota, Phys. Rev. B **61**, R2401 (2000); A. Janotti, R. Baierle, A. J. R. da Silva, R. Mota, and A. Fazzio, Physica B **273-274**, 575 (1999).